Cardiovascular Engineering and Technology, Vol. 10, No. 1, March 2019 *(© 2018)* pp. 61–68
https://doi.org/10.1007/s13239-018-00395-x

Objective Uniaxial Identification of Transition Points in Non-Linear Materials: Sample Application to Porcine Coronary Arteries and the Dependency of Their Pre- and Post-Transitional Moduli with Position

JENNY M. FREIJ, HANNA E. BURTON, and DANIEL M. ESPINO

Department of Mechanical Engineering, University of Birmingham, Birmingham B15 2TT, UK

(Received 21 February 2018; accepted 17 November 2018; published online 28 November 2018)

Associate Editors Dr. Ajit P. Yoganathan and Dr. Peter E. McHugh oversaw the review of this article.

Abstract
Purpose—This study aimed to develop an objective method for the elastic characterisation of pre- and post-transitional moduli of left anterior descending (LAD) porcine coronary arteries.
Methods—Eight coronary arteries were divided into proximal, middle and distal test specimens. Specimens underwent uniaxial extension up to 3 mm. Force–displacement measurements were used to determine the induced true stress and stretch for each specimen. A local maximum of the stretch-true stress data was used to identify a transition point. Pre- and post-transitional moduli were calculated up to and from this point, respectively.
Results—The mean pre-transitional moduli for all specimens was 0.76 MPa, as compared to 4.86 MPa for the post-transitional moduli. However, proximal post-transitional moduli were significantly greater than that of middle and distal test specimens ($p < 0.05$).
Conclusion—Post-transitional uniaxial properties of the LAD are dependent on location along the artery. Further, it is feasible to objectively identify a transition point between pre- and post-transitional moduli.

Keywords—Biomechanical testing/analysis, Connective tissues, Coronary artery, Mechanical properties, Young's modulus.

BACKGROUND

Coronary heart disease is the leading cause of death worldwide.[33] Characterising the mechanical properties of coronary arteries is important in order to determine stress and strain on the arterial wall[44] and is thus vital for clinical treatments of arterial diseases, designs of vascular implants (e.g. stents and grafts) as well as for tissue engineering.[21]

The coronary arteries are the first arterial branches of the aorta[41] with the main function of distributing oxygen at a high rate to the myocardium.[24] One of the two major branches of coronary circulation is the left coronary artery[26] of which the left anterior descending coronary artery (LAD) is of central importance.[21] The left coronary artery and its branches supply a majority of the oxygenated blood to the ventricular myocardium, as well as to the left atrium, left atrial appendage, pulmonary arteries and aortic root.[24] Coronary artery disease leads to chronic narrowing of the vessels or impaired vascular function which in turn can lead to cardiac hypoxia and impaired contractile function as well as increase the risk for a myocardial infarction.[26]

Mechanical testing has been performed on both human,[23,24,37,42] and porcine[29,42,44] coronary arteries. Porcine hearts are often chosen for their anatomical similarity to human hearts.[37] Uniaxial testing is a commonly chosen method for testing of coronary arteries,[21,29,37,42] with elastic material parameters often used in computational models.[19,28,29] However, a repeatable but objective measure of the pre- and post-transitional moduli following stress-stretch uniaxial testing is not currently available. There is the potential to use differences in post-transitional moduli to distinguish between healthy and diseased arteries[23]; with potential for clinical translation *via* elastography. Further, variations in these moduli along the length of the artery are unknown.

The aim of this study was to objectively measure the uniaxial behaviour of the left anterior descending coronary arteries of porcine hearts. Therefore, a method to identify the pre- and post-transitional

Address correspondence to Daniel M. Espino, Department of Mechanical Engineering, University of Birmingham, Birmingham B15 2TT, UK. Electronic mail: freij.jenny@gmail.com, h.e.burton@bham.ac.uk, d.m.espino@bham.ac.uk

moduli of arteries following uniaxial tests has been trialled. The methodology has been applied to proximal, middle and distal LAD coronary artery samples.

METHODS

Specimens

Eight coronary arteries were obtained from eight porcine hearts. The porcine hearts were delivered from a supplier (Fresh Tissue Supplies, Horsham, UK) who froze the hearts when excised and delivered them frozen and sealed. When delivered to the laboratory, the hearts were individually wrapped in tissue paper, soaked in Ringer's solution and then stored at − 40 °C in heat sealed bags. This followed protocols from previous studies involving porcine hearts.[10,11,14,34,45] Porcine hearts were thawed overnight at 4 °C, after which the LAD coronary artery was dissected from intact hearts. Each LAD coronary artery's length, width and thickness was measured before and after being divided into proximal, middle and distal test specimens, each 20.58 ± 0.75 mm in length (Fig. 1; Table 1). Specimens underwent a second freeze–thaw cycle ahead of uniaxial testing.

Uniaxial Testing

Test specimens were held in place using grips lined with emery paper. A piece of P400 emery paper with two rougher rectangular pieces of P60 emery paper, glued on using Araldite® Rapid (Huntsman Corporation, Texas, USA), was folded around the sample. Grips were attached to a Bose 3200 materials testing machine operated by WinTest software (Bose Corporation, ElectroForce Systems Group, Minnesota, USA). Each test specimen had a gauge length of 4.57 ± 0.75 mm. A thin piece of hydrated tissue paper was wrapped around the sample and re-hydrated with Ringer's solution between each cycle in order to avoid dehydration, as often performed for other soft connective tissues.[36,45]

Each sample underwent ten cycles of uniaxial testing, for each cycle it was stretched to a longitudinal displacement of 3 mm at a rate of 0.5 mm/s (i.e. tested axially), consistent with the longitudinal displacement of the left coronary artery[3,27] which ranges from 0.5 to 6.5 mm for the LAD.[3] Specimens were not tested to failure, as specimens were also used as part of a separate study.[5] Force–displacement data from the tenth, and final, cycle was used to calculate the pre- and post-transitional moduli (Fig. 2). The first nine cycles were used as preconditioning cycles, which coronary arteries require.[21,22,29,44]

Pre- and Post-Transitional Modulus

Coronary arteries typically display a 'J-shaped' curve during uniaxial tests,[7,28] by convention plotted as

TABLE 1. Dimensions of the LAD test samples.

	Proximal	Middle	Distal
Width (mm)	8.66 ± 1.03^{A}	6.90 ± 0.85^{B}	5.62 ± 0.63^{C}
Thickness (mm)	0.49 ± 0.08^{A}	0.34 ± 0.06^{B}	0.29 ± 0.10^{B}

The superscript letters A, B are used to indicate significant differences between the different regions; where regions do not share a letter they are significantly different ($p < 0.05$).

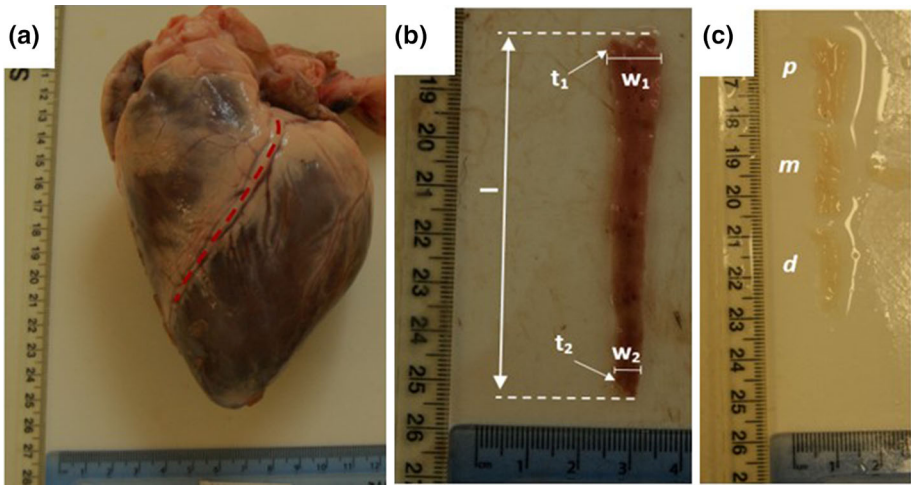

FIGURE 1. Porcine LAD coronary arteries. (a) Main dimensions to aid identification of full LAD sample length; (b) dissected coronary artery and surrounding myocardium; (c) proximal, p, middle, m, and distal, d, test samples obtained for testing. Measurements per sample included: sample longitudinal length (l), thickness (t_1 and t_2) and width of the specimens (W_1 and W_2). *Note*: (a) has been reproduced from Reference [5], which is distributed under the terms of the Creative Commons Attribution 4.0 International License (http://creativecommons.org/licenses/by/4.0/), which permits unrestricted use, distribution, and reproduction in any medium.

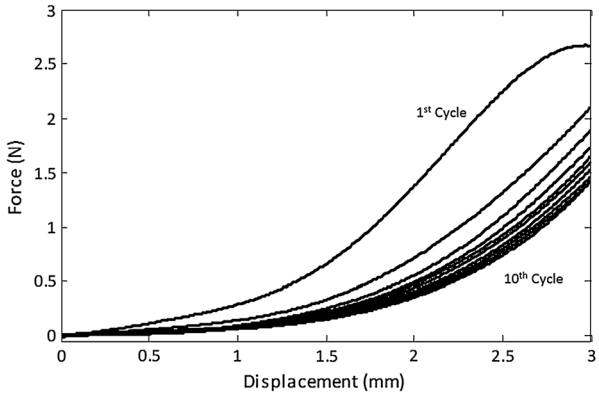

FIGURE 2. Ten force–displacement cycles for a coronary artery test specimen.

true stress, σ, over stretch, λ,[7,20,21,28,44] where λ is defined by Eq. (1) in terms of the actual length, l, and the initial length, L.[7,29] The initial length corresponded to the gauge length (see *Unaxial testing*, above) was used for calculations. Coronary arteries are considered to be incompressible,[18,19,23] so Eq. (2) is used to calculate the actual cross-sectional area, a, in relation to the initial cross-sectional area, A. Therefore, σ can be calculated using Eq. (3) based on the measured load, P, during testing.[7]

$$\lambda = \frac{l}{L} \tag{1}$$

$$a = \frac{A}{\lambda} \tag{2}$$

$$\sigma = \frac{P}{a} \tag{3}$$

The stress–stretch curve of coronary arteries contain what is commonly termed as a toe and a linear region[15,29,43] (Fig. 3). The stress–strain gradient within these toe and linear regions are defined as the pre- and post-transitional moduli, respectively. For this study, a critical point has been identified with corresponding stress, σ_C, and stretch, λ_C. This critical point, C in Fig. 3, was defined by identifying the critical point closest to the origin (for λ, $\sigma > 0$) of the estimated polynomial regression line of the data plotted as the stretch over true stress. A third-degree polynomial regression line has been used. This is because it was the lowest degree polynomial which led to a suitable goodness of fit ($R^2 = 85.65 \pm 9.19\%$). Further, it was the only regression trendline which consistently displayed an identifiable local maximum at the transition point. This local maximum was identifiable when the data was plotted as the stretch over true stress (Fig. 3). Thus, this is an essential part of this method; the use of lower order polynomials, for example, did not always lead to such an identifiable point. The critical point stretch, λ_C, was used to identify a corresponding stretch (up to two significant figures) on the actual experimental data which had been plotted. The result was a transition stretch, λ_T. λ_T is necessary because λ_C does not necessarily match a data point on the stress-stretch curve; λ_T is identified as the nearest data stretch point to λ_C. The transition stretch, together with the corresponding transition true stress, σ_T, formed the transition point (λ_T, σ_T), point T in Fig. 3. In essence, T is the mapping of C from the polynomial regression line on to the experimental data. Subsequently, the pre- and post-transitional moduli were calculated using point T as an end and start point for each, respectively.

Statistical Analysis

The pre- and post-transitional moduli were analysed with respect to the LAD geometry. Width and thickness of the samples were compared to the distance from the bifurcation, the post-transitional modulus was compared to the width of the samples. Regression analysis was performed with SigmaPlot (v12.0, Systat Software Inc., USA). Minitab (v17, Minitab Inc., USA) was used to assess statistical significance for one-way ANOVA ($p < 0.05$) between the geometry of the proximal, middle and distal test specimens. Statistically significant differences ($p < 0.05$) were also analysed between matched pre- and post-transitional moduli, the storage and loss moduli using a paired t test.

RESULTS

The proximal, middle and distal samples had a mean width of 8.66 ± 1.03 mm, 6.90 ± 0.85 mm and 5.62 ± 0.63 mm (Table 1), respectively, and decreased significantly along the distance from the bifurcation ($p < 0.05$, $R^2 = 70.91\%$; Fig. 4). The thickness of the proximal, middle and distal pieces were 0.49 ± 0.08 mm, 0.34 ± 0.06 mm and 0.29 ± 0.10 mm (Table 1), respectively, again decreasing significantly along the distance from the bifurcation ($p < 0.05$, $R^2 = 53.15\%$; Fig. 4).

There was a statistically significant difference between pre- and post-transitional moduli (Table 2). The average pre-transitional modulus ranged from 0.67 MPa for proximal samples to 0.85 MPa for the distal samples; whereas, post-transitional moduli ranged from 2.62 MPa (distal) to 8.06 MPa (proximal). However, there was no statistically significant difference between the stretch at which the transition point occurred for the proximal, middle or distal samples.

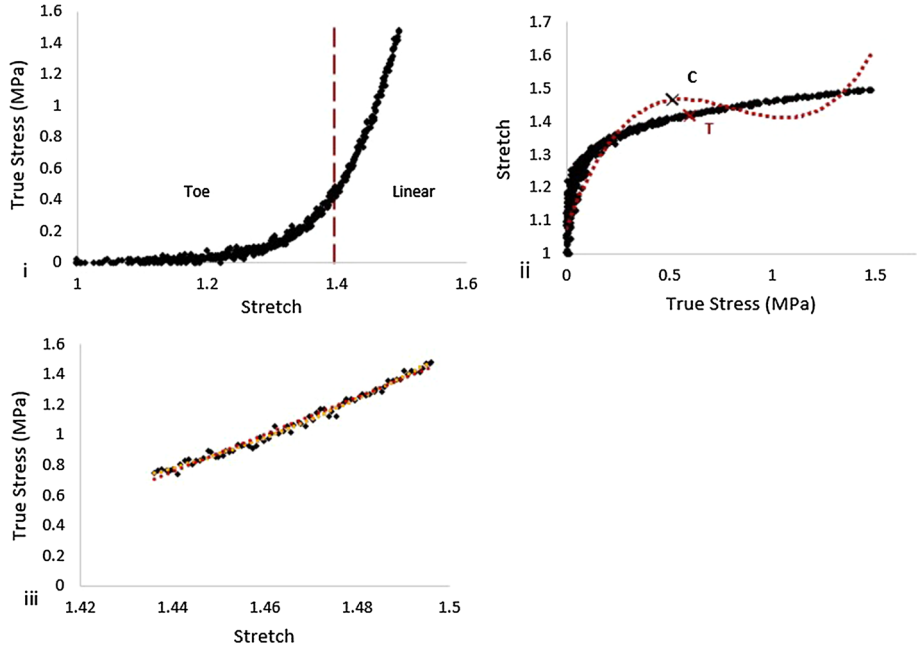

FIGURE 3. Objective methodology for determining pre- and post-transitional moduli, including a transition point between the two. The typical true stress (MPa) over stretch plot (i) is inverted so as to plot stretch-true stress (ii) and a third degree regression line is used to identify a local maximum referred to as the critical point, *C*, from which the nearest stretch data point is identified as the transition point, *T*. The pre-transitional and post-transitional (iii) moduli are then calculated up to and starting from *T*, respectively. Linear (red) and quadratic (yellow) relationships have been assessed.

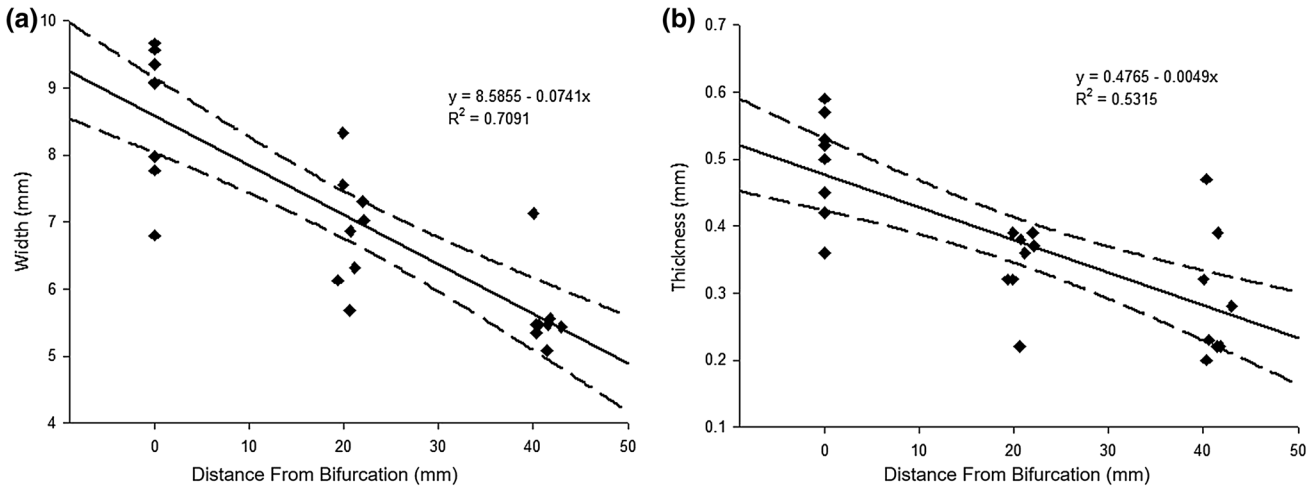

FIGURE 4. Variation of LAD (a) width and (b) thickness along the artery (distance from the bifurcation). Regression analysis (solid line) includes 95% confidence intervals (dashed lines) and the 95% confidence intervals (dashed lines); note, both relationships were significant ($p < 0.05$).

The average transition point occurred at $\lambda = 1.53 \pm 0.11$.

There was no significant difference between the pre-transitional moduli at different distances from the bifurcation (Table 2). The overall mean pre-transitional modulus was 0.76 ± 0.38 MPa. While a linear relationship was used to calculate this modulus, regression analysis shows that a quadratic fit (Eq. 4) provided a better fit for the data (Table 3). Constants from Eq. (4) for proximal, middle and distal samples are provided in Table 4.

$$\sigma = \alpha\lambda^2 - \beta\lambda + \gamma \tag{4}$$

The mean post-transitional modulus for all test specimens was 4.86 MPa. However, there was a statistically significant difference in post-transitional moduli between proximal (8.06 MPa) and middle (3.90 MPa) or distal (2.62 MPa) samples (Table 2). There was little

TABLE 2. Mean ± SD (standard deviation) of pre- and post-transitional moduli for proximal, middle and distal LAD samples.

	Pre-transitional (MPa)	Post-transitional (MPa)
Proximal	$0.67 \pm 0.30^{A*}$	8.06 ± 1.56^{A}
Middle	$0.77 \pm 0.29^{A*}$	3.90 ± 1.47^{B}
Distal	$0.85 \pm 0.53^{A*}$	2.62 ± 2.96^{B}
Mean	0.76 ± 0.38	4.86 ± 2.84

The superscript letters A, B are used to indicate significant differences between the different regions; where regions do not share a letter they are significantly different ($p < 0.05$).
*Indicates a statistically significant difference ($p < 0.05$) between pre- and post-transitional modulus.

TABLE 3. Regression analysis for linear and quadratic relationships between pre- and post-transitional true stress–stretch data (mean ± SD).

	Linear R^2 (%)	QUADRATIC R^2 (%)
Pre-transitional	61.7 ± 11.2	89.9 ± 13.6
Post-transitional	93.8 ± 5.5	95.0 ± 5.6

TABLE 4. Constants (in MPa) defining a pre-transitional true-stress stretch quadratic relationship (Eq. 4).

	α	β	γ	R^2 (%)
Proximal	2.42	5.19	2.75	98
Middle	3.37	7.17	3.79	98
Distal	3.48	7.70	4.19	89
Mean	3.22	6.99	3.75	76

difference in R^2 values for linear (94%) and quadratic (95%) σ–λ relationships (Table 3). The post-transitional modulus was also found to increase significantly ($p < 0.05$, Fig. 5) with thickness and width, however, R^2 values were low at 26 and 30%, respectively.

DISCUSSION

An objective method has been trialled to measure the pre- and post-transitional moduli for proximal, middle and distal samples of the LAD coronary artery. The post-transitional modulus varied across the length of the coronary artery and with the thickness of the LAD. Unsurprisingly, there is a significant difference between the pre- and post-transitional moduli of the LAD coronary artery. More importantly it was feasible to identify a transition point, mathematically, to distinguish between pre- and post- transitional components of the true stress-stretch curve.

The proximal post-transitional moduli from this study are consistent with the range of values available in literature, ranging from around 1.5 MPa[23] up to 10 MPa.[29] However, the identification of the point from where this post-transitional region starts is vaguely defined in previous studies.[23,29] Lower values of around 0.1 MPa have also been reported in the literature.[28,32] However, such findings are based on biaxial tests and there are difficulties in comparing between uniaxial and biaxial testing methodologies. Thus, although the sample size used in this study could be considered low, the results obtained in our study are consistent with available literature. Further our sample size exceeds that of other studies in literature.[25]

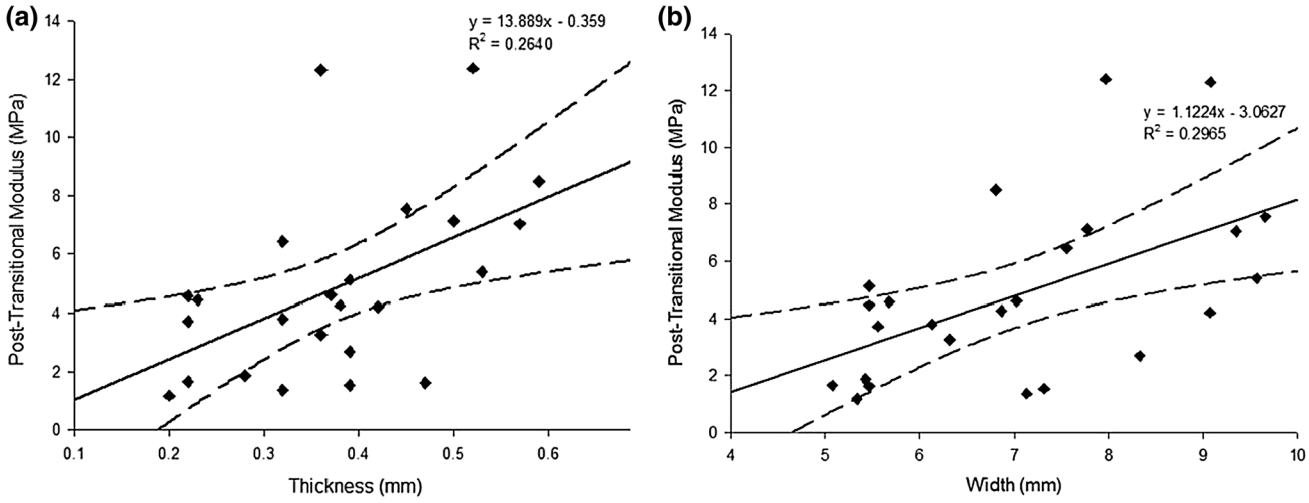

FIGURE 5. Regression analysis of the dependency of post-transitional modulus on (a) thickness and (b) width. Regression analysis (solid line) includes 95% confidence intervals (dashed lines) and the 95% confidence intervals (dashed lines); note, both relationships were significant ($p < 0.05$).

The method used to calculate and identify the pre- and post-transitional modulus, although novel, is based on there being an identifiable transition point between the pre- and post-transition of a stretch-stress curve of a coronary artery.[7] Considering the advantages of using a linear fit compared to a quadratic one in determining a pre- and post-transitional modulus, the use of a linear fit is thus considered of greater value. For example, implementation of a single pre- and/or post-transitional modulus simplifies the implementation in using computational models.[12,13] However, it is noted that this may introduce some limitations in terms of the pre-transitional modulus which is best represented by a quadratic σ–λ relationship.

The lumen diameter of LAD has been previously documented. Dodge *et al.*[9] and Zhang *et al.*[46] observed the proximal and distal lumen diameter of human LAD coronary artery to be 3.7 mm and 3.92 mm as well as 1.9 mm and 2.10 mm, respectively. Leung *et al.*[31] measured the proximal human LAD lumen diameter to vary between 3.30 and 3.88 mm and Guo *et al.*[17] found the inner lumen diameter of porcine LAD to vary between 2.19 and 0.02 mm. During this study, the width of the LAD was measured when the specimen had been cut open to resemble a rectangular specimen. Thus, the measured widths, w, from our current study is a measure of the inner circumference of the artery. Assuming a circular cross-section, means that the outer diameter, d_o, measured in other studies would be approximately equivalent to

$$d_o = \frac{w}{\pi} + 2t \tag{6}$$

here, t is the wall thickness. Thus, outer diameters for proximal, middle and distal samples were 3.7, 2.9 and 2.4 mm, respectively. Although the measured width of the proximal section of the LAD in this study are consistent with those by Dodge *et al.*[9] and Leung *et al.*[31] other comparisons are hard to make since the location of the distal section is not always clear.[38] Measurements might also vary between human[46] and porcine specimens. Geometrical considerations are important because our study found that post-transitional moduli decreased with LAD thickness and, thus, along the artery.

A limitation of this study is that samples have undergone freeze–thaw cycles. Briefly, while freeze–thaw cycles might influence tissue mechanics to some extent, it is the method of freezing which is critical[2,16,35]; as discussed elsewhere in more detail.[5] Microscopic assessment of coronary arteries using the freeze–thaw protocols employed in this study have found limited effect on their structure.[6] Ultimately, the agreement of our data with literature suggests that it has not impaired the mechanics of the tissues assessed. Furthermore, as the overall stress–strain trend has not been altered by this process, it does not limit the assessment of an objective method for identifying a transition point. Such a transition point has potential uses clinically, in terms of distinguishing between pre- and post-transitional moduli. These moduli can be useful on their own in terms of enabling distinction between healthy and diseased arteries[23] with potential applications to magnetic resonance elastography[40] for diagnosis. Alternatively, they may enable the identification of linear regions (i.e. post-transitional) for more advanced characterisation, such as dynamic viscoelasticity of arteries,[5] heart valves,[4] and other tissues, replacement materials[30,39] and/or chemically treated natural tissues.[8] Ahead of implementation on a wide range of materials, the authors would suggest that any test data used is consistent with existing recommendations for test data to be suitable for characterisation, e.g.[1] This is because any characterisation method will be sensitive to the range of input data, and their spacing, as the parameters of acquisition/sampling can disproportionately bias subsequent fits (altering subsequent coefficients determined through characterisation).

CONCLUSION

It is feasible to identify a transition point from a pre- to a post-transitional modulus of soft connective tissues. Using this objective method, the post-transitional modulus of porcine left anterior descending coronary arteries was found to decrease along its proximal–distal length.

AUTHORS' CONTRIBUTIONS

JMF participated in the study's design, performed mechanical testing and drafted the initial manuscript. HEB conceived the study, participated in its design, and edited the manuscript. DME conceived the study, participated in its design, and edited the manuscript. All authors read and approved the final manuscript.

CONFLICT OF INTEREST

The authors declare that they have no conflict of interest.

ETHICAL APPROVAL

No animals were sacrificed specifically for this study. Porcine hearts were supplied by Fresh Tissue Supplies (Horsham, UK). Ethical approval was

granted for this study by the University of Birmingham Research Support Group [ERN_15-0032].

ACKNOWLEDGMENTS

The authors would like to thank the Engineering and Physical Sciences Research Council for the studentship for HEB [EP/M114612B]. The equipment used in this study was funded by Arthritis Research UK [H0671].

REFERENCES

[1]Abaqus version 6.10. Abaqus Analysis User's Manual; Part V: Materials. Providence: Dassault Systemes Simulia Corporation, 2010.

[2]Aidulis, D., D. E. Pegg, C. J. Hunt, Y. A. Goffin, A. Vanderkelen, B. van Hoeck, *et al*. Processing of ovine cardiac valve allografts: 1. Effects of preservation method on structure and mechanical properties. *Cell Tissue Bank* 3:79–89, 2002.

[3]Arbab-Zadeh, A., A. N. DeMaria, W. F. Penny, R. J. Russo, B. J. Kimura, and V. Bhargava. Axial movement of the intravascular ultrasound probe during the cardiac cycle: implications for three-dimensional reconstruction and measurements of coronary dimensions. *Am. Heart J.* 138:865–872, 1999.

[4]Baxter, J., K. G. Buchan, and D. M. Espino. Viscoelastic properties of mitral valve leaflets: an analysis of regional variation and frequency-dependency. *Proc. Inst. Mech. Eng. Part H J. Eng. Med.* 231:938–944, 2017.

[5]Burton, H. E., J. M. Freij, and D. M. Espino. Dynamic viscoelasticity and surface properties of porcine left anterior descending coronary arteries. *Cardiovasc. Eng. Technol.* 8:41–56, 2017.

[6]Burton, H. E., R. L. Williams, and D. M. Espino. Effects of freezing, fixation and dehydration on surface roughness properties of porcine left anterior descending coronary arteries. *Micron* 101:78–86, 2017.

[7]Claes, E., Atienza, J., Guinea, G., Rojo, F., Bernal, J., Revuelta, J., et al. Mechanical properties of human coronary arteries. Engineering in Medicine and Biology Society (EMBC). In: 2010 Annual International Conference of the IEEE, IEEE, 2010, pp. 3792–3795.

[8]Constable, M., H. E. Burton, B. M. Lawless, V. Gramigna, K. G. Buchan, and D. M. Espino. Effect of glutaraldehyde based cross-linking on the viscoelasticity of mitral valve basal chordae tendineae. *Biomed. Eng. Online* 17:93, 2018.

[9]Dodge, J., B. G. Brown, E. L. Bolson, and H. T. Dodge. Lumen diameter of normal human coronary arteries. Influence of age, sex, anatomic variation, and left ventricular hypertrophy or dilation. *Circulation* 86:232–246, 1992.

[10]Espino, D. M., D. W. L. Hukins, D. E. T. Shepherd, M. A. Watson, and K. G. Buchan. Determination of the pressure required to cause mitral valve failure. *Med. Eng. Phys.* 28:36–41, 2006.

[11]Espino, D. M., D. E. T. Shepherd, and K. G. Buchan. Effect of mitral valve geometry on valve competence. *Heart Vessels* 22:109–115, 2007.

[12]Espino, D. M., D. E. T. Shepherd, and D. W. L. Hukins. Development of a transient large strain contact method for biological heart valve simulations. *Comput. Methods Biomech. Biomed. Eng.* 16:413–424, 2013.

[13]Espino, D. M., D. E. T. Shepherd, and D. W. L. Hukins. Evaluation of a transient, simultaneous, arbitrary Lagrange–Euler based multi-physics method for simulating the mitral heart valve. *Comput. Methods Biomech. Biomed. Eng.* 17:450–458, 2014.

[14]Espino, D. M., D. E. T. Shepherd, D. W. L. Hukins, and K. G. Buchan. The role of chordae tendineae in mitral valve competence. *J. Heart Valve Dis.* 14:603–609, 2005.

[15]Freed, A. D., and T. C. Doehring. Elastic model for crimped collagen fibrils. *J. Biomech. Eng.* 127:587–593, 2005.

[16]Goh, K. L., Y. Chen, S. M. Chou, A. Listrat, D. Bechet, and T. J. Wess. Effects of frozen storage temperature on the elasticity of tendons from a small murine model. *Animal* 4:1613–1617, 2010.

[17]Guo, X., Y. Liu, and G. S. Kassab. Diameter-dependent axial prestretch of porcine coronary arteries and veins. *J. Appl. Physiol.* 112:982–989, 2012.

[18]Holzapfel, G. A. Biomechanics of soft tissue. In: The Handbook of Materials Behavior Models: Nonlinear Models and Properties, edited by J. Lemaitre. France: Academic Press, 2010.

[19]Holzapfel, G. A., T. C. Gasser, and M. Stadler. A structural model for the viscoelastic behavior of arterial walls: continuum formulation and finite element analysis. *Eur. J. Mech. A Solids* 21:441–463, 2002.

[20]Holzapfel, G. A., and R. W. Ogden. Constitutive modelling of arteries. *Proc. R. Soc. A Math. Phys. Eng. Sci.* 466:1551–1597, 2010.

[21]Holzapfel, G. A., G. Sommer, C. T. Gasser, and P. Regitnig. Determination of layer-specific mechanical properties of human coronary arteries with nonatherosclerotic intimal thickening and related constitutive modeling. *Am. J. Physiol. Heart Circ. Physiol.* 289:H2048–H2058, 2005.

[22]Humphrey, J. D. Cardiovascular solid mechanics: cells, tissues, and organs. New York: Springer, 2002.

[23]Karimi, A., M. Navidbakhsh, A. Shojaei, and S. Faghihi. Measurement of the uniaxial mechanical properties of healthy and atherosclerotic human coronary arteries. *Mater. Sci. Eng. C Mater. Biol. Appl.* 33:2550–2554, 2013.

[24]Katz, A. M. Physiology of the Heart (5th ed.). Philadelphia: Lippincott Williams & Wilkins, 2010.

[25]Khoffi, F., and F. Heim. Private mechanical degradation of biological heart valve tissue induced by low diameter crimping: an early assessment. *J. Mech. Behav. Biomed. Mater.* 44:71–75, 2015.

[26]Klabunde, R. Cardiovascular Physiology Concepts (2nd ed.). Philadelphia: Lippincott Williams & Wilkins, 2011.

[27]Konta, T., J. Hugh, and N. Bett. Patterns of coronary artery movement and the development of coronary atherosclerosis. *Circulation* 67:846–850, 2003.

[28]Kural, M. H., M. Cai, D. Tang, T. Gwyther, J. Zheng, and K. L. Billiar. Planar biaxial characterization of diseased human coronary and carotid arteries for computational modeling. *J. Biomech.* 45:790–798, 2012.

[29]Lally, C., A. Reid, and P. Prendergast. Elastic behavior of porcine coronary artery tissue under uniaxial and equibiaxial tension. *Ann. Biomed. Eng.* 32:1355–1364, 2004.
[30]Lawless, B. M., S. C. Barnes, D. M. Espino, and D. E. T. Shepherd. Viscoelastic properties of a spinal posterior dynamic stabilisation device. *J. Mech. Behav. Biomed. Mater.* 59:519–526, 2016.
[31]Leung, W. H., M. L. Stadius, and E. L. Alderman. Determinants of normal coronary artery dimensions in humans. *Circulation* 84:2294–2306, 1991.
[32]Lu, X., A. Pandit, and G. S. Kassab. Biaxial incremental homeostatic elastic moduli of coronary artery: two-layer model. *Am. J. Physiol. Heart Circ. Physiol.* 287:H1663–H1669, 2004.
[33]Mackay, J., and G. A. Mensah. The Atlas of Heart Disease and Stroke. Geneva: World Health Organization, 2004.
[34]Millard, L., D. M. Espino, D. E. T. Shepherd, D. W. L. Hukins, and K. G. Buchan. Mechanical properties of chordae tendineae of the mitral heart valve: young's modulus, structural stiffness, and effects of aging. *J. Mech. Med. Biol.* 11:221–230, 2011.
[35]Muller-Schweinitzer, E. *Cryopreservation of vascular tissues. Organogen.* 5:97–104, 2009.
[36]Öhman, C., M. Baleani, and M. Viceconti. Repeatability of experimental procedures to determine mechanical behaviour of ligaments. *Acta Bioeng. Biomech.* 11:19–23, 2009.
[37]Ozolanta, I., G. Tetere, B. Purinya, and V. Kasyanov. Changes in the mechanical properties, biochemical contents and wall structure of the human coronary arteries with age and sex. *Med. Eng. Phys.* 20:523–533, 1998.
[38]Perry, R., M. X. Joseph, D. P. Chew, P. E. Aylward, and C. G. De Pasquale. Coronary artery wall thickness of the left anterior descending artery using high resolution transthoracic echocardiography—normal range of values. *Echocardiography* 30:759–764, 2013.
[39]Sadeghi, H., D. M. Espino, and D. E. T. Shepherd. Variation in viscoelastic properties of bovine articular cartilage below, up to and above healthy gait-relevant loading frequencies. *Proc. Inst. Mech. Eng. Part H J. Eng. Med.* 229:115–123, 2015.
[40]Thomas-Seale, L. E. J., L. Hollis, D. Klatt, I. Sack, N. Roberts, P. Pankaj, and P. R. Hoskins. The simulation of magnetic resonance elastography through atherosclerosis. *J. Biomech.* 49:1781–1788, 2016.
[41]Townsend Jr, C. M., R. D. Beauchamp, B. M. Evers, and K. L. Mattox. Sabiston Textbook of Surgery (19th ed.). Philadelphia: Elsevier, 2012.
[42]Van Andel, C. J., P. V. Pistecky, and C. Borst. Mechanical properties of porcine and human arteries: implications for coronary anastomotic connectors. *Ann. Thorac. Surg.* 76:58–64, 2003.
[43]Venkatasubramanian, R. T., E. D. Grassl, V. H. Barocas, D. Lafontaine, and J. C. Bischof. Effects of freezing and cryopreservation on the mechanical properties of arteries. *Ann. Biomed. Eng.* 34:823–832, 2006.
[44]Wang, C., M. Garcia, X. Lu, Y. Lanir, and G. S. Kassab. Three-dimensional mechanical properties of porcine coronary arteries: a validated two-layer model. *Am. J. Physiol. Heart Circ. Physiol.* 291:H1200–H1209, 2006.
[45]Wilcox, A. G., K. G. Buchan, and D. M. Espino. Frequency and diameter dependent viscoelastic properties of mitral valve chordae tendineae. *J. Mech. Behav. Biomed. Mater.* 30:186–195, 2014.
[46]Zhang, L., D. Xu, X. Liu, X. S. Wu, Y. N. Ying, Z. Dong, *et al.* Coronary artery lumen diameter and bifurcation angle derived from CT coronary angiographic image in healthy people. *Chin. J. Cardiol.* 39:1117–1123, 2011.